Data driven three-phase Fundamental Diagram for traffic modeling

Jiah Song, jiahsong@umich.edu
Department of Mathematics, University of Michigan

Romesh Saigal, rsaigal@umich.edu
Department of Industrial and Operations Engineering, University of Michigan

Kang-Ching Chu, kcchu@umich.edu
Department of Mechanical Engineering, University of Michigan

Qi Luo, luoqi@umich.edu
Department of Industrial and Operations Engineering, University of Michigan

May 31, 2016

ABSTRACT

Macroscopic traffic flow models are widely used to estimate traffic status on a freeway, and the fundamental diagram (FD), that establishes a relationship between density and flux, is essential for these models to be effective. By visualizing the 2005 traffic trajectory data from Next Generation SIMulation (NGSIM) project on US Highway 101 and Interstate 80 in California, we observed three states of traffic condition: free flow, mildly congested flow, and highly congested flow; and the resulting shockwaves. The FD is critical in understanding the shockwave phenomenon of congested flow. Therefore, there is a need to develop a more accurate FD that captures the complexity of the density-flux relation observed in the empirical data. For this we develop a three phase FD of traffic flow.

In our previous work, a log piecewise linear FD was shown to fit better than some other forms of FD on 2009 traffic data from Interstate 95 in Virginia. However, the previous FD considered two phases, free and congested flow. The three phase modification we propose here is able to distinguish between the highly and the mildly congested flow and explains the resulting shockwaves. The phase transition from mildly to highly congested state changes the nature of the flux-density function from a concave to a convex function of density. In the concave phase a forward moving and in the convex phase a backward moving shock results. This FD can also explain the rarefaction waves that arise in traffic flow.

NGSIM data covers every vehicle within its range and we focus our study to the innermost lane. The visualized data is used to fit the three phases. This involved solving an optimization problem to determine the values of the parameters. A close relationship between the backward shockwaves during highly congested phase and the convex part of the FD is observed. A single parameter value (slope of the log-linear function) is shown to predict the various conditions of the traffic: free, mildly and highly congested flow.

The proposed FD can be used in conjunction with any macroscopic traffic flow model, such as LighthillWhithamRichards (LWR), for traffic flow estimation with greatly improved accuracy. A three-phase FD and a stochastic macroscopic traffic flow model can reliably predict future traffic status, and provide advanced information to drivers and transportation authorities for travel planning, traffic management, and other real-time applications.

1 INTRODUCTION

The performance of transportation system is crucial to economy and living quality of a community. In 2014, traffic congestion in the US caused drivers 6.9 billion hours of extra time sitting in the traffic and resulted in a congestion cost of $160 billion according to Schrank et al. (*1*). Managing traffic and controlling congestion require an accurate estimation of traffic flow evolution. While macroscopic traffic flow models and microscopic simulation tools are two main approaches for traffic state estimation and prediction, because of their lower computational costs, macroscopic models are favored for real-time application. Also macroscopic models can provide approximate traffic status efficiently using scarce data collected from stationary detectors or trajectory data from individual vehicles.

In macroscopic traffic flow, three variables, the flux (Q), the density (ρ) and the average velocity/speed (v), where $Q = \rho v$, are considered. The fundamental diagram (FD) is used to model the relationship between density and flux. In addition, traffic flow is typically divided into two states, free flow and congested flow, and it is particularly challenging to model congested flow since the dynamics of congested traffic is more complex. Traffic shockwave phenomenon has been clearly observed in the congested flow by Kerner (*2*), and a third phase called wide moving jam is defined to distinguish it from typical congested traffic. For a macroscopic model to capture this phenomenon, an explicit expression between flux and density (i.e. the FD) which sufficiently explains the occurrence of traffic shock waves is required.

This paper presents a newly defined three-phase FD of traffic flow, where the objective is to distinguish the formation and propagation of traffic shockwaves. The next section introduces the required traffic theory background and an overview of the literature, followed by the proposed model and theory. In the RESULTS section, two different sets of vehicle trajectory data from Next Generation SIMulation, NGSIM (*3*), are used to validate proposed three-phase FD, as well as the effectiveness of applying this model in analyzing traffic shock waves through the observation of a

single parameter m. The last section states the conclusion of the presented work and proposes future work and possible applications.

2 BACKGROUND AND RELATED WORK

The simple yet insightful LWR (Lighthill and Whitham (*4*), Richards (*5*)) model has been the building block of macroscopic traffic flow models since its first appearance in 1955. The classical LWR model, a nonlinear first order partial differential equation, treats traffic flow as a compressible fluid and studies properties induced by the interaction of a group of vehicles. Although the LWR model fails to explain several minor phenomena, such as hysteresis and traffic oscillations, indicated by Li et al. (*6*), its hydrodynamic approach that implements mass conservation in traffic flow is valid for homogeneous traffic flow. Many efforts have been made to improve LWR model, such as including higher order term, adding source terms to flow conservation, and considering stochastic nature of traffic. Some of the widely accepted higher order models include Payne (*7*), Aw and Rascle (*8*), and Zhang (*9*). Yang et al. (*10*) proposed a stochastic partial differential equation model building on the classic LWR traffic flow model to capture the variation of congestion and gradual revert to the mean values after any random perturbations.

The LWR model allows discontinuous solutions in a weak sense and produces the generation and propagation of traffic shock waves. The speed of the shock wave, denoted by s, for a jump from ρ_L to ρ_R is

$$s = \frac{Q(\rho_R) - Q(\rho_L)}{\rho_R - \rho_L} \tag{1}$$

by the Rankine-Hugoniot condition, LeVeque (*11*). Here ρ_R represents the density to the right of the shock, and ρ_L to the left of the shock. The shock speed s in (1) can be either positive or negative, and this results in either forward-moving shock or backward-moving shock. It has been widely recognized that the Oleinik entropy condition is required in order to pick the physically

relevant weak solution among multiple weak solutions. The details regarding entropy-satisfying shock with our proposed flux-density relation will be described in the next section.

Besides traffic theories based on physics, sensor technology and the development of intelligent transportation system allow researchers to use traffic data from real traffic and computer simulations to better understand traffic phenomenon. Based on a thorough analysis using empirical data from German freeways, Kerner (*2*) proposed the three-phase traffic theory. Rather than a single congestion state, congested traffic is divided into two phases, synchronized flow and wide moving jam. According to Kerner's definition, synchronized flow is when vehicles are continuously moving under high density traffic, with possibly no significant drop in flux. On the other hand, wide moving jam is caused by sudden drop in velocity with very high traffic density, and the jam moves backwards across the space.

In macroscopic traffic models, vehicles can maintain constant velocity when density is low (free flow), so the flux increases with density. In traffic with higher density the velocity decreases and the flux may also decrease. The fundamental diagram (FD) captures this phenomenon with the flux-density relationship. Other than the basic triangular FD, several forms of the FD have been proposed in the past, and some of these have been frequently used in the literature. For example, Greenshields et al. (*12*) considered a linear speed-density relationship as $v_f(1-\rho/\rho_j)$ with free-flow velocity v_f and critical density ρ_j as parameters. Also, Greenberg (*13*) proposed a logarithmic relationship as $v_0 \ln(\rho_j/\rho)$ and Underwood (*14*) used exponential form, $v_f \exp(-\rho/\rho_j)$. Since some FDs are more appropriate for congested traffic while others are more suitable for free flow, it is possible to mix them in application by adopting one in congested sections and another in the free-flow sections. Yang et al. (*10*) proposed the log piecewise linear function to express speed-density relation, which has been tested and shown to have the best fit among models mentioned above in both free flow and congested flow regimes. Lu et al. (*15*) investigated a lane-wise FD and proposed variable structure models with two limbs of the inverse $\lambda-$shape and a special generalized polynomial model for the right limb. Although Kerner (*2*) argues that there is no

unique flux-density relationship in Kerner's three-phase traffic theory, Treiber et al. (*16*) showed that macroscopic traffic model with FD is capable of representing three-phase traffic. Daganzo and Geroliminis (*17*) also pointed out that FD is not expected universally due to several factors that dramatically affects the performance of congested flow in traffic.

Even for the stochastic traffic flow model with log piecewise linear FD used by Yang et al. (*10*) and Chu et al. (*18*), the two-phase FD did not successfully reflect the complexity of traffic congestion including traffic shock waves. This deficiency of the FD motivated us to modify the log piecewise linear FD using the concept of three-phase traffic flow similar to Kerner's theory, and this allows phase transitions to be clearly defined by the range of a single exponent value in fundamental relation formula.

3 MODEL AND THEORY

Throughout this paper, the following notation is used:

- (x, t) is the space and time, respectively.
- $Q(x, t)$ is the flux, number of vehicles per unit time at location x and time t.
- $\rho(x, t)$ is the density, number of vehicles per unit distance at location x and time t.
- $v(x, t)$ is the average velocity of all vehicles at location x and time t.

In the rest of this paper, the independent variables (x, t) are omitted from the notation.

3.1 Three-Phase Fundamental Diagram

The LWR model consists of the scalar conservation law of mass (2) and the relationship among Q, ρ and v, known as the fundamental relation of traffic flow (3),

$$\frac{\partial \rho}{\partial t} + \frac{\partial Q}{\partial x} = 0 \quad \text{and} \tag{2}$$

$$Q = \rho \cdot v. \tag{3}$$

On a freeway, the vehicles tend to drive at some optimal velocity. That is to say, they drive at high speed in light traffic and they slow down in heavy traffic. Therefore the velocity is dependent on the local density. This additional information leads to the definition of Q, which is a well-defined function of the conserved quantity ρ. The fundamental diagram (FD) of traffic flow describes this relationship between Q and ρ. It plays an important role in the use of the LWR model. Therefore, to have a good predictive model, the FD should reflect the 'true' relationship as accurately as possible.

In our previous work, a log piecewise linear FD (4) was shown to fit better than some other forms of FD on 2009 traffic data from Interstate 95 in Virginia, Yang et al. (*10*). This model takes the form of

$$v = \min\{v_f,\ \alpha\rho^m\} \tag{4}$$

where v_f refers to the free flow velocity, $m < 0$ and α is a constant. However, this original model considered two phases, free and congested flow. In order to distinguish between the highly and the mildly congested flow, we develop a *modified* log piecewise linear model that includes three different phases. The *modified* model is

$$v = \min\{v_f,\ \alpha^*\rho^{m^*},\ \bar{\alpha}\rho^{\bar{m}}\} \tag{5}$$

where $\bar{m} < -1 < m^* < 0$, α^* and $\bar{\alpha}$ are constants, and v_f refers to the free flow velocity. This is called a *modified log piecewise* linear model because (5) takes a piecewise linear form (see (7)) in a logarithm manner. It has been observed that m is negative in the original model, Yang et al. (*10*), and we divide this m into two parameters, m^* and $\bar{m}$, by a critical value -1 in the modified model, which makes Q turn from concave to convex as a function of ρ. The key idea of the critical

value -1 came from the observation of backward-moving shockwave in traffic flow and

$$\frac{\partial \rho}{\partial t} + \alpha(m+1)\rho^m \frac{\partial \rho}{\partial x} = 0 \tag{6}$$

obtained by manipulating (2) and (3). In (6), note that the information propagates to the left when $m < -1$, which results in the backward-moving shockwaves.

Now we describe our three-phase traffic flow in detail from the observation by visualizing the data, motivated by and similar to Kerner's three-phase traffic theory but with different definitions.

- The first or the free-flow phase ($m = 0$): This is when v is near the speed limit. In this phase, we observe that v is not affected by ρ.

- The second or the mildly congested phase ($-1 < m^* < 0$): We observed the presence of data showing that traffic congestion begins to occur, that is, v decreases as ρ increases. In particular, this data shows the slow-down behavior is not as abrupt as in traffic jam. Note that in a logarithm form, (5) takes

$$\ln v = \min\{\ln v_f,\ \ \ln \alpha^* + m^* \ln \rho,\ \ \ln \bar{\alpha} + \bar{m} \ln \rho\}, \tag{7}$$

  so the negative slope in the (log) phase plane, $\ln v$ vs $\ln \rho$, is in between 0 and 1 in magnitude. This is how $-1 < m^* < 0$ was derived in this second phase. Moreover, in this mildly congested flow, Q still increases as a concave function of ρ. We also claim that this phase is where the forward-going shock may occur. This will be discussed in the next subsection.

- The third or the highly congested phase ($\bar{m} < -1$): As ρ increases more and more, we observed that v decreases quite abruptly. This results in the slope (in $\ln v$ and $\ln \rho$ plane, see (7)) being less than -1. Quantitatively this is where $\bar{m} < -1$ came from. This sudden slow-down behavior generates a shock that propagates backwards in space as time evolves.

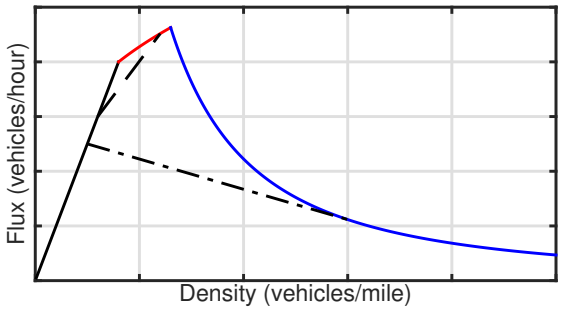

Figure 1: The three-phase fundamental diagram. The dashed line is related to a forward-moving shock and the dash-dot line is related to a backward-moving shock.

While Q increases in the mildly congested phase, Q in this highly congested phase decreases as a convex function of ρ.

FIGURE 1 illustrates the proposed three-phase FD; Q is an increasing linear function of ρ in the first phase (black). Q is an increasing and concave function of ρ in the second phase (red) while Q is a decreasing and convex function of ρ in the third phase (blue). We note that this three-phase FD is not concave unlike the majority of proposed FD in the literature is concave.

3.2 **Entropy Satisfying/Violating Shocks and Compound Waves**

It is well known that the weak solutions of (2) are not in general unique, so the physically relevant solution should be selected somehow and one way is to check the entropy condition. For more details of non-uniqueness of weak solutions, we refer the reader to LeVeque (*11*). Furthermore, due to the fact that the three-phase FD has a shape of non-convexity, we should expect to have Riemann solutions with possibly both a shock and rarefaction fan. So in this subsection, we discuss entropy-satisfying/violating shocks and compound waves. Note that the shock speed s in (1) can be either positive or negative, which results in either *forward-moving* or *backward-moving shock*.

- *Forward-moving shock* : In mildly congested flow, a vehicle slows down due to the behavior of its preceding vehicle, and this effect continues to the following vehicle. Hence, the disturbance propagates backwards in space through the lines of vehicle trajectories (this is the main reason

why drivers do not notice the forward-going shock wave) while a rise in ρ may propagate forward in space. Within the three-phase FD, several possibilities of forward-moving shock may be considered when $\rho_L < \rho_R$. First, if ρ_L in the first phase jumps into ρ_R in the second phase, then the Oleinik entropy condition is satisfied:

$$\frac{Q(\rho_L) - Q(\rho)}{\rho_L - \rho} \geq \frac{Q(\rho_L) - Q(\rho_R)}{\rho_L - \rho_R} \tag{8}$$

for all ρ between ρ_L and ρ_R. The dashed line in FIGURE 1 illustrates such forward-moving shock. Second, if ρ_L in the second phase jumps into ρ_R in the second phase, then (8) is also satisfied. Third, if ρ_L in the first phase jumps into ρ_R in the third phase, then (8) is satisfied only when $Q(\rho_L) < Q(\rho_R)$. Lastly, if ρ_L in the second phase jumps into ρ_R in the third phase, then (8) is also satisfied only in a very limited case when $Q(\rho_L) < Q(\rho_R)$. Phase transition in ρ may or may not be necessary for the forward-moving shock to be realized, which is summarized in solid lines in FIGURE 2.

- *Backward-moving shock* : While the forward-moving shock is hardly observed in reality, backward-moving shocks are easily observed. Within the three-phase FD, when ρ_R is in the third phase and ρ_L is in the first phase as in the dash-dot line in FIGURE 1, the shock propagates backwards in space due to the negative speed of the shock s in (1) (case 1). For example, in a situation where the traffic is going fast, when the lead vehicle suddenly slows down for some reason, ρ of following vehicles increases with a sudden slowdown. So there is a jump in the value of ρ and this jump travels backwards in space. This single jump could be represented as in the dash-dot line in FIGURE 1. In addition to that, ρ_R is in the third phase and ρ_L in the second phase as in the red heavy line in FIGURE 3, the shock also propagates backwards in space (case 2). In both cases, the entropy-satisfying shock propagates backwards in space, provided that $Q(\rho_R) < Q(\rho_L)$ under the Oleinik entropy condition (8). These are also summarized in dashed lines in FIGURE 2.

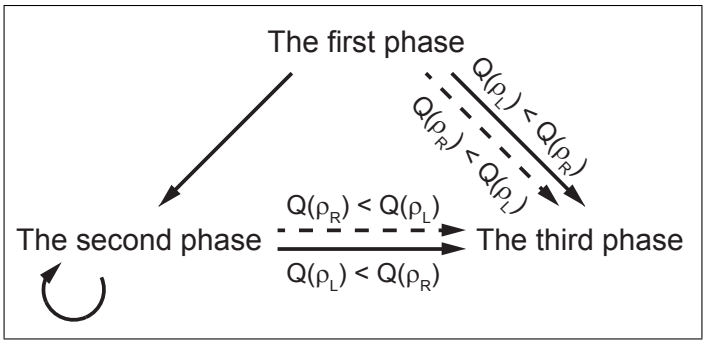

Figure 2: Phase transitions when shock in density is generated. Solid lines imply the forward-moving shock while dashed lines imply the backward-moving shock.

- *Entropy-violating shock* : With the three-phase FD, an entropy-violating shock wave can arise. When both ρ_L and ρ_R are in the third phase and $\rho_L < \rho_R$, it is expected that a backward-propagating shock wave is created. However, this violates the Entropy condition as we can see from (8). This prediction of the three-phase FD needs explanation and is to be investigated and researched further.

- *Compound waves* : When considering a non-convex flux function, it is known that the Riemann solution might involve both a shock and a rarefaction wave. We present an example of this. Taking the case of ρ_L in the third phase and ρ_R in the second phase like the situation along the red dotted line in FIGURE 3, the Riemann solution will contain both a rarefaction and a shock propagating backwards. This illustrates that ρ suddenly drops from ρ_L to some value of density through a shock wave and then to ρ_R through a rarefaction.

4 DATA FITTING AND OPTIMIZATION OF PARAMETER m

The traffic dataset used in this paper to fit and validate the three-phase fundamental diagram (FD) was collected under the Next Generation SIMulation (NGSIM (*3*)) project. Datasets from the inner-most lane of US Highway 101 (US 101) and the lane 2 of Interstate 80 (I-80) were used. US 101 data records vehicle trajectories and instantaneous velocity on the southbound of US 101 in Los Angeles, CA, between 7:50 a.m. and 8:05 a.m. on June 15, 2005. The study

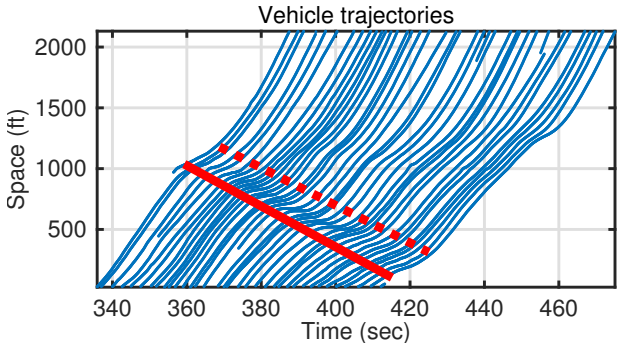

Figure 3: Vehicle trajectories of the NGSIM (US 101) around 7:55 a.m. to 7:57 a.m. on June 15th, 2005, along with backward-moving shock area (red line) and rarefaction wave area (red dotted line).

area is approximately 2,100 feet in length. The I-80 data of vehicle trajectories was recorded on northbound direction of Interstate 80 in San Francisco, CA, between 4:00 p.m. and 4:15 p.m. on April 13, 2005. The site is approximately 1,650 feet in length. Both (US 101 and I-80) vehicle trajectory data provided the precise location of each vehicle within the study area every one-tenth of a second with detailed lane positions. The following subsections contain two types of results: the FD generated from the fitting of the speed-density relationship (i.e. the modified log piecewise linear function) and the result of optimized parameter m.

4.1 **Data fitting of Three-Phase Fundamental Diagram**

In this subsection, we present the result of fitting of (7), which is the modified log piecewise linear model. First, average velocity was calculated by the mean of recorded velocity data every 18 seconds and 50 feet and the FIGURE 4 (a) shows the average velocity of trajectory data of US 101. Flux was calculated by counting the number of vehicles in every 18 seconds. Then density was computed by (3).

The fitting result of the speed-density relation in logarithm form and the corresponding FD are presented in FIGURE 5. The FD is not universally expected according to Daganzo and Geroliminis (*17*), and consequently it changes as region changes. In this context, two different regions in US 101 data (region A and region B in FIGURE 4 (a)) were selected to fit the modified

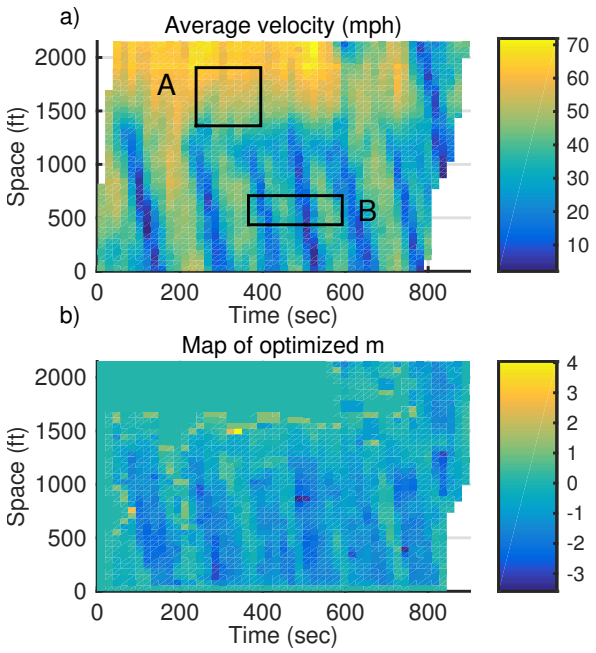

Figure 4: (a) Average velocity of 15 minutes (7:50 a.m. to 8:05 a.m.) of US 101 on June 15th, 2005. (b) Optimized m.

piecewise linear function in a log form. Piecewise linear regression was applied to fit the data (after taking the logarithm) in each of two regions A and B and to estimate each parameter (α, m). By doing this, the data in each regions were segregated into two sections by a critical density, ρ_c, which is determined by minimizing the sum of squares of the differences between observed and computed ln(speed). The critical densities were turned out to be $\rho_c^* = 24.7543$ in region A as in FIGURE 5 (b) and $\bar{\rho}_c = 51.5731$ in region B as in FIGURE 5 (d). The fitted results for the first and the second phases in region A are as follows:

$$\ln v = 4.0618 \quad \text{and} \tag{9}$$

$$\ln v = -0.5588 \cdot \ln \rho + 5.857, \tag{10}$$

where (9) is shown as a black linear line and (10) is a red linear line in FIGURE 5 (a). FIGURE 5 (b) demonstrates the corresponding FD that provides the first and the second phases of the three-

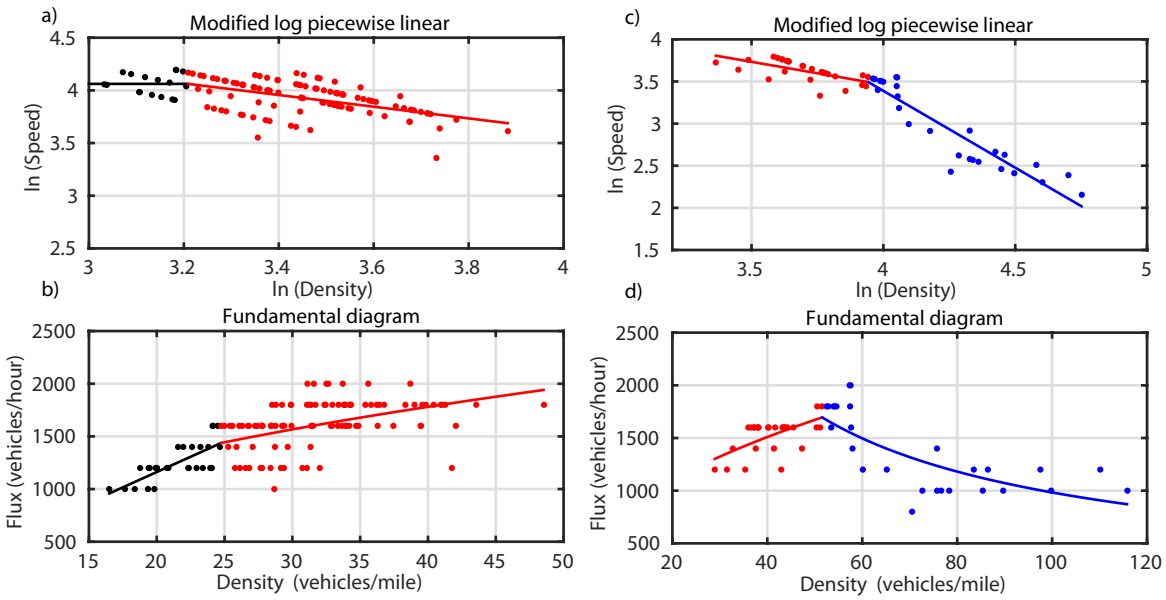

Figure 5: (a) The first and second phases of the three-phase flow on the modified log piecewise linear function in the region A of US 101 data. (b) The first and second phases of the three-phase flow on the fundamental diagram of traffic flow in the region A of US 101 data. (c) The second and third phases of the three-phase flow on the modified log piecewise linear function in the region B of US 101 data. (d) The second and third phases of the three-phase flow on the fundamental diagram of traffic flow in the region B of US 101 data.

phase flow as we expected from FIGURE 1. The fitted results for the second and third phases in region B are as follows:

$$\ln v = -0.542 \cdot \ln \rho + 5.63 \quad \text{and} \tag{11}$$

$$\ln v = -1.823 \cdot \ln \rho + 10.68, \tag{12}$$

where (11) is shown as a red linear line and (12) is a blue linear line in FIGURE 5 (c). FIGURE 5 (d) demonstrates the corresponding FD that provides the second and the third phases of the three-phase flow as we also expected from FIGURE 1. As we observed backward-moving shocks in region B from FIGURE 4 (a), the fitted result in FIGURE 5 (d) provides $\bar{m} < -1$ that is relevant to negative speed of shock. Moreover, putting data in region A and B together, we obtained the three-phase FD shown in FIGURE 6 as proposed in FIGURE 1. The Table 1 lists the fitted results

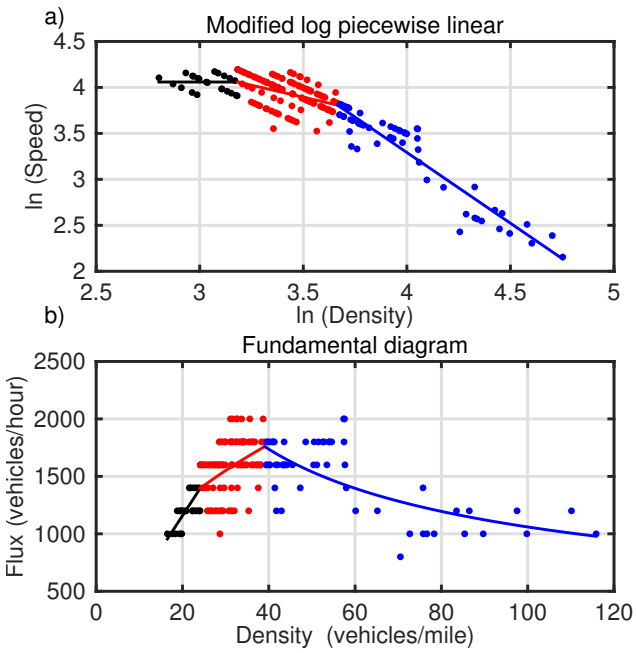

Figure 6: (a) The three phases of the modified log piecewise linear function in the combined region A and B of US 101 data. (b) The three-phase fundamental diagram of traffic flow in the combined region A and B of US 101 data.

Table 1: Regression result of modified log piecewise linear model of US 101 data

Region	**Phase**	**m**	$\ln \alpha$	$\mathbf{R^2}$
A	2	-0.5588	5.857	0.2689
B	2	-0.542	5.63	0.4191
	3	-1.823	10.68	0.8558
A and B combined	2	-0.5486	5.814	0.1978
	3	-1.536	9.436	0.8901

of the modified log piecewise linear function in region A, region B, and the combined region. For the fitting of combined region, the low R^2 in the second phase is due to the mixed data from two different regions. The critical densities turned out to be 24.1190 (vehicles/mile) which separates the first phase from the second phase and 39.0561 (vehicles/mile) which separates the second phase from the third phase.

The same procedure was performed to I-80 dataset. The average velocity of recorded

trajectory data of I-80 is presented in FIGURE 8 (a). This average velocity was calculated by the mean of recorded velocity data every 9 seconds and 25 feet. The result of fiiting of the speed-density function and the FD are presented in FIGURE 8 (c) and (d) with the second and third phases. The first phase was not included because the average velocity ranges from 0 to approximately 37 mph as seen in FIGURE 8 (a). Fitted results of the modified piecewise linear function for I-80 dataset in region C illustrated in FIGURE 8 (a) are shown in Table 2 and FIGURE 8 (c). The critical density turned out to be 105.2144 (vehicles/mile) in region C.

4.2 **Optimization of parameter m**

In this subsection, we attempt to optimize m over the entire space-time domain in order to identify the role of parameter m. To find the optimized m for US 101 data, the space-time plane was discretized by choosing a mesh width $\Delta x = 50$ (feet) and a time step $\Delta t = 18$ (sec), and defined the discrete mesh points (x_i, t_j) by $x_i = i\Delta x$ and $t_j = j\Delta t$. The parameter m was optimized based on the assumption that change in density in the future on a highway depends on the past (backward in time) information and the surrounding environment of drivers (centered in space). Namely, $m(x_i, t_j)$ is dependent upon $v(x_{i+k}, t_{j+l})$ and $\rho(x_{i+k}, t_{j+l})$ for $k = -1, 0, 1$, and $l = -2, -1, 0$ where $m(x_i, t_j)$ indicates numerical value of m at the discrete grid point (x_i, t_j). And then we found

$$\arg \min_{m,\alpha} \| \ln v - m \ln \rho - \ln \alpha \|_2^2.$$

The result of the optimized m of US 101 data is shown in FIGURE 4 (b). We can interpret that m being -1 is a threshold that distinguishes the third phase from the second phase. On one hand, the region where $m = \bar{m} < -1$ appears to be the third phase, and clearly there exists a shock traveling backwards in space. On the other hand, in the region where $-1 < m = m^* < 0$, there appears to be the second phase. FIGURE 7 (a) depicts the region at where $-1 < m = m^* < 0$ and FIGURE 7 (b) illustrates the region at where $m = \bar{m} < -1$. A visual validation is followed by

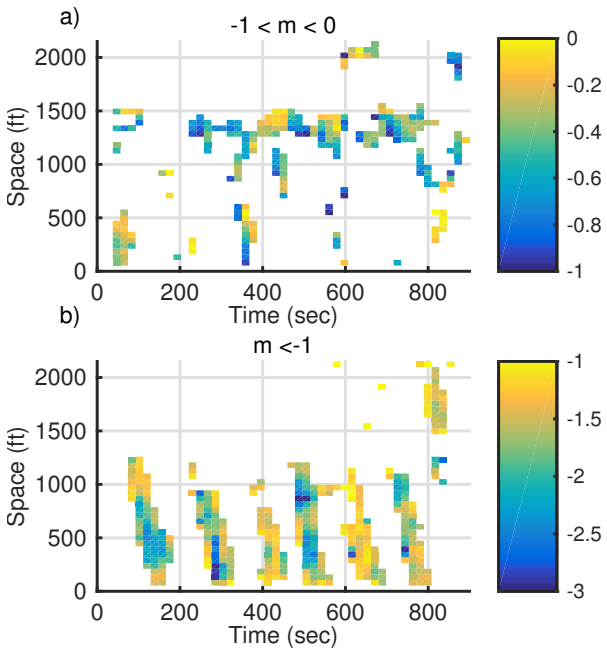

Figure 7: (a) Optimized m only when $-1 < m < 0$ for US 101 data. (b) Optimized m only when $m < -1$ for US 101 data.

Table 2: Regression result of modified log piecewise linear model of I-80 data

Region	**Phase**	**m**	$\ln \alpha$	$\mathbf{R^2}$
C	2	-0.6699	5.889	0.4795
	3	-1.742	10.88	0.8655

comparing the map of optimized m (in FIGURE 4 (b)) with the average velocity (in FIGURE 4 (a)). The result of the optimized m of I-80 data is also shown in FIGURE 8 (b) (we used $\Delta x = 25$ (feet) and $\Delta t = 9$ (sec)). As we can see from those results, the value of m gives an indication of how congested the traffic is. Again, the fact that the optimized m in FIGURE 8 (b) and the average velocity in FIGURE 8 (a) match up well enough provides us a visual validation.

5 CONCLUSION

This paper presents a new approach to the three-phase fundamental diagram (FD) in macroscopic traffic flow based on visualization of 2005 traffic trajectory data from Next Generation SIMulation

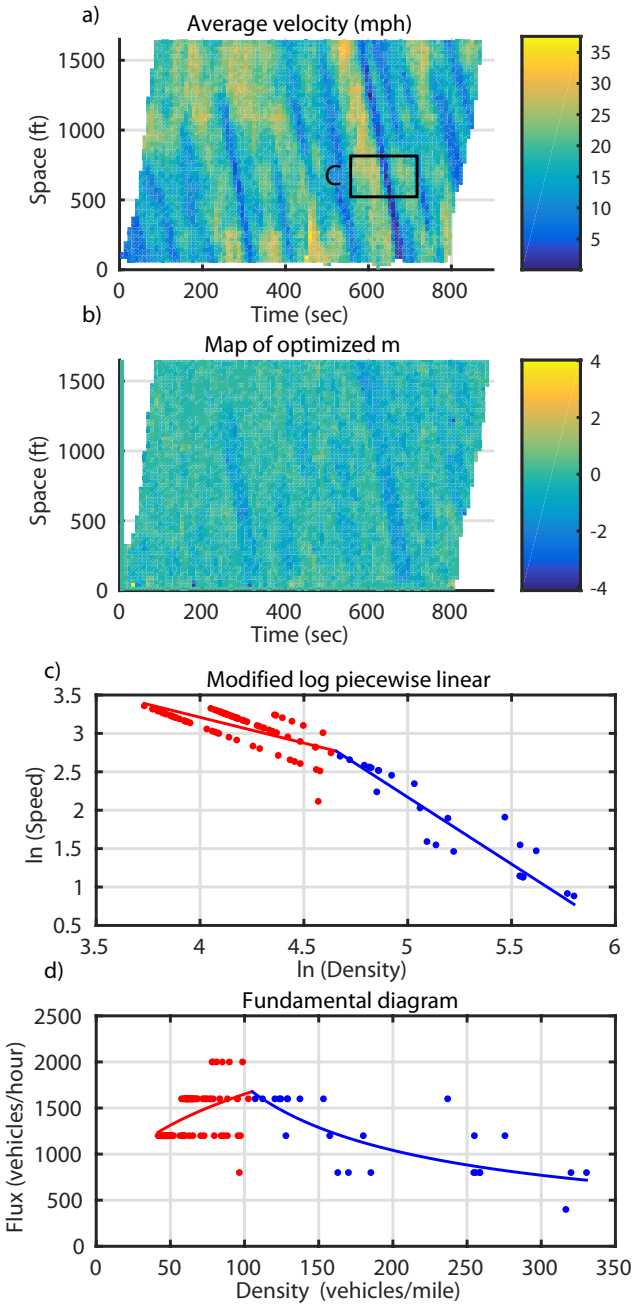

Figure 8: (a) Average velocity of 15 minutes (4:00 p.m. to 4:15 p.m.) of I-80 on June 15th, 2005. (b) Optimized m. (c) The second and third phases of the three-phase flow on the modified log piecewise linear function in the region C of I-80 data. (d) The second and third phases of the three-phase flow on the fundamental diagram of traffic flow in the region C of I-80 data.

(NGSIM) project on US Highway 101 and Interstate 80 in California. The result shows that the proposed three-phase FD is capable of capturing three different phases (free, mildly and highly

congested flow), and it clearly shows the change in concavity in the FD. Furthermore, the single parameter m, slope of the log-linear function, plays a crucial role as an indication to differentiate the second phase from the third phase, and the critical m turns out to be -1.

The reason that the fit in the second phase is relatively poor compared to the fit in the third phase could be the high variabilities in the second phase, which is not well captured by the model we proposed. In our future work, we will use the LWR model or other appropriate macroscopic traffic flow models along with the three-phase FD or possibly introduce stochasticity to capture randomness of data and driver behavior to reliably predict future traffic status.

REFERENCES

[1] Schrank, D., B. Eisele, T. Lomax, and J. Bak, Urban mobility scorecard. *Technical Report August, Texas A&M Transportation Institute and INRIX, Inc*, 2015.

[2] Kerner, B. S., Three-phase traffic theory and highway capacity. *Physica A: Statistical Mechanics and its Applications*, Vol. 333, 2004, pp. 379–440.

[3] NGSIM, *Next Generation Simulation http://ngsim-community.org/, US Department of Transportation*, 2005.

[4] Lighthill, M. J. and G. B. Whitham, On kinematic waves. II. A theory of traffic flow on long crowded roads. In *Proceedings of the Royal Society of London A: Mathematical, Physical and Engineering Sciences*, The Royal Society, 1955, Vol. 229, pp. 317–345.

[5] Richards, P. I., Shock Waves on the Highway. *Operations Research*, Vol. 4, No. 1, 1956, pp. 42–51.

[6] Li, J., Q.-Y. Chen, H. Wang, and D. Ni, Analysis of LWR model with fundamental diagram subject to uncertainties. *Transportmetrica*, Vol. 8, No. 6, 2012, pp. 387–405.

[7] Payne, H. J., Models of freeway traffic and control. *Mathematical models of public systems*, 1971.

[8] Aw, A. and M. Rascle, Resurrection of "second order" models of traffic flow. *SIAM journal on applied mathematics*, Vol. 60, No. 3, 2000, pp. 916–938.

[9] Zhang, H. M., A non-equilibrium traffic model devoid of gas-like behavior. *Transportation Research Part B: Methodological*, Vol. 36, No. 3, 2002, pp. 275–290.

[10] Yang, L., R. Saigal, C.-P. Chu, and Y.-W. Wan, Stochastic model for traffic flow prediction and its validation. In *Transportation Research Board 90th Annual Meeting*, 2011, 11-0086.

[11] LeVeque, R. J., *Numerical methods for conservation laws*, Vol. 132. Springer, 1992.

[12] Greenshields, B., J. Bibbins, W. Channing, and H. Miller, A study of traffic capacity. In *Highway Research Board Proceedings*, 1935.

[13] Greenberg, H., An analysis of traffic flow. *Operations Research*, Vol. 7, No. 1, 1959, pp. 79–85.

[14] Underwood, R., Speed, volume, and density relationships: Quality and theory of traffic flow. *Yale Bureau of Highway Traffic, New Haven, CT*, 1961, pp. 141–188.

[15] Lu, X.-Y., P. Varaiya, and R. Horowitz, Fundamental Diagram modeling and analysis based NGSIM data. In *12th IFAC Symposium on Control in Transportation System*, 2009, pp. 367–374.

[16] Treiber, M., A. Kesting, and D. Helbing, Three-phase traffic theory and two-phase models with a fundamental diagram in the light of empirical stylized facts. *Transportation Research Part B: Methodological*, Vol. 44, No. 8-9, 2010, pp. 983–1000.

[17] Daganzo, C. F. and N. Geroliminis, An analytical approximation for the macroscopic fundamental diagram of urban traffic. *Transportation Research Part B: Methodological*, Vol. 42, No. 9, 2008, pp. 771–781.

[18] Chu, K.-C., L. Yang, R. Saigal, and K. Saitou, Validation of stochastic traffic flow model with microscopic traffic simulation. In *2011 IEEE Conference on Automation Science and Engineering (CASE)*, 2011, pp. 672–677.